Excitation-Contraction Coupling Gain and Cooperativity of the Cardiac Ryanodine Receptor: A Modeling Approach

Kai Wang,* Yuhai Tu,† Wouter-Jan Rappel,* and Herbert Levine*
*Department of Physics and Center for Theoretical Biological Physics, University of California at San Diego, La Jolla, California; and †IBM T.J. Watson Research Center, Yorktown Heights, New York

ABSTRACT During calcium-induced calcium-release, the ryanodine receptor (RyR) opens and releases large amounts of calcium from the sarcoplasmic reticulum into the cytoplasm of the myocyte. Recent experiments have suggested that cooperativity between the four monomers comprising the RyR plays an important role in the dynamics of the overall receptor. Furthermore, this cooperativity can be affected by the binding of FK506 binding protein, and hence, modulated by adrenergic stimulation through the phosphorylating action of protein kinase A. This has important implications for heart failure, where it has been hypothesized that RyR hyperphosphorylation, resulting in a loss of cooperativity, can lead to a persistent leak and a reduced sarcoplasmic-reticula content. In this study, we construct a theoretical model that examines the cooperativity via the assumption of an allosteric interaction between the four subunits. We find that the level of cooperativity, regulated by the binding of FK506 binding-protein, can have a dramatic effect on the excitation-contraction coupling gain and that this gain exhibits a clear maximum. These findings are compared to currently available data from different species and allows for an evaluation of the aforementioned heart-failure scenario.

INTRODUCTION

Congestive heart failure (HF) is a condition affecting more than two million people in the United States, characterized by reduced contractility of the heart muscle (1–3). Many of these patients will die directly from this contractile dysfunction, associated with a reduction of calcium transients elicited in response to electrical stimulation; others will die from ventricular arrhythmias, many of which themselves appear related to this calcium handling malfunction (4). The calcium transient reduction, in turn, appears to be primarily due to a decrease in the amount of releasable calcium in the sarcoplasmic reticulum (SR) (5). Many factors can contribute to this reduction, including lowered SERCA pump activity, smaller influx through the L-type channel, anomalous activity of the sodium-calcium exchanger and, of concern here, increased SR leak through the ryanodine receptor (RyR) array. The relative importance of these components continues to be debated (3,6,7).

In this study, we focus on the role of RyR subunit cooperativity as it affects RyR gating and hence diastolic SR leak. Initial evidence for this cooperativity came from lipid bilayer experiments in which the concentration of FK506-binding protein (FKBP) was controlled (8,9). The RyR, a homotetramer comprised of four monomers that can each bind one FKBP, was found to exhibit subconductance states in the absence of FKBP. These subconductance states are characterized by fractional openings of the receptor and the current through these fractional openings were, interestingly, either one-quarter, one-half, or three-quarters of the current of a fully opened channel. The clear implication of this in vitro data was that FKBP binding induced a coupling between the otherwise independent opening and closing dynamics of the individual subunits.

Data from isolated myocyte studies also shows the importance of FKBP in RyR functioning. However, these experiments provide seemingly contradictory results: sequestering of FKBP in rats (10) and mice (11) was found to increase excitation-contraction (E-C) coupling gain, whereas in rabbits it resulted in a decreased E-C coupling gain (12). In addition, overexpression of FKBP in rabbits was reported to increase the calcium transient and contractility (13,14), whereas overexpression in rats decreased the spontaneous spark frequency, while increasing the calcium transient (15).

To model the role of FKBP in RyR gating, we introduce an allosteric interaction between the RyR subunits whose strength is modulated by FKBP binding. This interaction changes the transition rates in a Markov process approach to RyR gating. We find that the E-C coupling gain exhibits a clear maximum for a certain optimal level of cooperativity (i.e., an optimal value of FKBP binding). In addition, we find that an increase in cooperativity leads to a decrease in the spontaneous spark frequency. These results are then critically compared to existing experimental data. Furthermore, our model can be compared to detailed information regarding the effects of adrenergic stimulation, based on the fact that stimulation leads to activation of cAMP-dependent protein kinase A (PKA), which then lowers FKBP binding via RyR phosphorylation (16,17).

It is through the action of PKA that HF is hypothesized to lead to increased SR leak. Specifically, a chronic hyperadrenergic state during HF leads to elevated levels of PKA and consequently the RyR becomes hyperphosphorylated (18,19). This leads to a persistent dissociation of FKBP and

Submitted January 10, 2005, and accepted for publication August 5, 2005.

Address reprint requests to H. Levine, Tel.: 858-534-4844; E-mail: hlevine@ucsd.edu.

0006-3495/05/11/3017/09 $2.00

doi: 10.1529/biophysj.105.058958

presumably a reduced SR content (19–21). Our results lend support to this proposed mechanism, as we show that a reduction of cooperativity as would be caused by FKBP disassociation would indeed give rise to a large RyR leak and a concomitantly reduced SR content. Although one obviously needs to use a more comprehensive model to account for all the changes in calcium handling one would expect under HF conditions, the results to-date do show that this idea is quantitatively sensible.

We note in passing a final set of experiments that link FKBP directly to cardiac arrhythmias: FKBP deficient mice were found to consistently exhibit exercise-induced ventricular arrhythmias and sudden cardiac death (22), most likely caused by delayed after-depolarization resulting from calcium mishandling. Moreover, it was shown that restoring the binding of FKBP through pharmaceutical intervention was able to protect these mice from ventricular arrhythmias (23). Although it remains extremely challenging to relate subcellular-scale physiology with organism scale response, we view this latest work as an indication that properly modeling the effects of FKBP is a critical issue that is timely to address.

MATERIALS AND METHODS

Intracellular calcium dynamics

The calcium dynamics in the myocyte is locally controlled through the tight coupling between the L-type calcium channels and the RyR cluster. In our model, the calcium concentration in the dyadic space, $[Ca^{2+}]_{ds}$, is described as

$$\frac{d[Ca^{2+}]_{ds}}{dt} = J_{RyR} + J_{dhpr} + J_{buf} - \frac{[Ca^{2+}]_{ds} - [Ca^{2+}]_{cyto}}{\tau_{efflux}}. \quad (1)$$

Here, J_{buf} describes the binding of calcium to buffers that are present in the dyadic space (24),

$$J_{Buf} = -\sum_j k_{j,on}[Ca^{2+}]_{ds}([B_j] - [CaB_j]) - k_{j,off}[CaB_j]. \quad (2)$$

The sum is over three calcium buffers B (calmodulin, SR membrane buffers, and sarcolemmal membrane buffers) of constant concentration. For a full description including parameter settings, we refer to the Supplementary Material. Furthermore, J_{RyR} is the flux through the RyRs, J_{dhpr} is the L-type channel flux, and the last term represents the flow of calcium ions from the dyadic space to the cytoplasm.

The equation for the calcium concentration in the junctional SR (jSR), $[Ca^{2+}]_{jSR}$, includes the release of calcium through the RyR receptors and the refilling from the network SR (nSR), where the calcium concentration, $[Ca^{2+}]_{nSR}$, is taken as constant,

$$\frac{d[Ca^{2+}]_{jSR}}{dt} = \beta_{jSR}\left(-\frac{V_{ds}}{V_{jSR}}J_{RyR} + \frac{[Ca^{2+}]_{nSR} - [Ca^{2+}]_{jSR}}{\tau_{refill}}\right), \quad (3)$$

where the parameter values are listed in Table 1. In this equation, we have assumed rapid equilibrium between calcium and calsequestrin in the junctional SR, leading to (25)

$$\beta_{jSR} = \left(1 + \frac{[B_{CSQN}]K_{CSQN}}{(K_{CSQN} + [Ca^{2+}]_{ds})^2}\right)^{-1}. \quad (4)$$

TABLE 1 Cell geometry parameters

Parameter	Description	Value	Reference
A_{cap}	Cell capacitance	153.4 pF	(26)
V_{cyto}	Cytoplasm volume	25.84 pL	(26)
V_{jSR}	Junctional SR volume	0.16 pL	(26)
V_{nSR}	Network SR volume	2.1 pL	(26)
V_{ds}	Dyadic space volume	1.2×10^{-3} pL	(26)
$[Ca^{2+}]_o$	Extracellular calcium concentration	2.0 mM	(26)
$[Ca^{2+}]_i$	Cytosolic calcium concentration	0.1 μM	(24)
$[Ca^{2+}]_{nSR}$	Network SR calcium concentration	1.0 mM	(24)
τ_{efflux}	Dyadic space efflux time	7.0×10^{-7} s	(24)
τ_{refill}	Junctional SR refilling time	0.003 s	(25)

In most of the simulation results reported here, we assumed that $[Ca^{2+}]_{cyto}$ was constant and equal to its resting cytosolic calcium concentration $[Ca^{2+}]_i$. Furthermore, the nSR calcium concentration $[Ca^{2+}]_{nSR}$ was also taken constant. These assumptions lead to a more computationally tractable model that avoids the simulation of the cytosolic calcium machinery including SERCA pumps and the sodium-calcium exchanger. Furthermore, since $[Ca^{2+}]_{nSR}$ is assumed to be constant, it is sufficient to simulate a single calcium-release unit (CRU) (see Simulation Protocol, below). However, we have also performed simulations using a full model in which these assumptions are relaxed. Details of this model can be found in the Supplementary Material. The results of these simulations (shown in Fig. 4) demonstrate that the full model produces qualitatively identical results to the simple model.

The L-type calcium channel

To model the L-type channel, we adopt the formulation from Iyer et al. (26), along with its parameters. The channel is described via a Markov model consisting of 11 voltage and calcium-dependent states along with two voltage-dependent inactivation states. The calcium current through a single channel can be written as

$$I_{dhpr} = P_{Ca}\frac{4VF^2}{RT}\frac{[Ca^{2+}]_{ds}e^{2VF/RT} - 0.341[Ca^{2+}]_o}{e^{2VF/RT} - 1}, \quad (5)$$

leading to a total flux through the L-type channel

$$J_{dhpr} = -\frac{N_{open,dhpr}I_{dhpr}}{2FV_{ds}}, \quad (6)$$

where V is the membrane potential, P_{Ca} is the channel permeability, $[Ca^{2+}]_o$ is the extracellular calcium concentration, and where $N_{open,dhpr}$ is the number of open L-type calcium channels, which is at most 10-per-CRU in our simulation. For further details, we refer to Greenstein and Winslow (25) and Iyer et al. (26).

The RyR

As already noted, the RyR is a homotetramer comprised of four monomers that can each bind one FKBP. Lipid bilayer experiments have shown that RyR can exhibit one-quarter, one-half, and three-quarters of the total channel conductance when FKBP is absent (8). In our model, we thus assume that each subunit can be activated upon binding of one calcium ion and is responsible for one-quarter of the maximum current via a conformational change. To model the gating kinetics of the subunits, we will employ a simple scheme in which each subunit can be in one of three states: closed (C), open (O), or inactivated (I) (see Fig. 1). Similar gating schemes, but

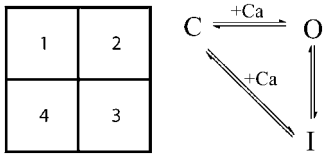

FIGURE 1 (*Left*) A schematic picture of the RyR used in our model. Each receptor consists of four subunits that only interact with its nearest-neighbor (i.e., subunit *1* interacts with subunits *2* and *4*, but not with subunit *3*). (*Right*) The three-state model for each RyR subunit.

without subunit coupling, were investigated in Stern et al. (27). To incorporate the FKBP binding effect, we assume that it can introduce an allosteric energy between neighboring subunits and that subunits are energetically penalized for being in a different state than their neighbors. This allosteric energy is introduced via a symmetric energy matrix with vanishing diagonal terms:

$$\mathbf{\Delta E} = s \times \begin{pmatrix} 0 & \Delta E_{\rm co} & \Delta E_{\rm ci} \\ \Delta E_{\rm co} & 0 & \Delta E_{\rm oi} \\ \Delta E_{\rm ci} & \Delta E_{\rm oi} & 0 \end{pmatrix}. \tag{7}$$

The continuous variable s is the key parameter in our model and controls the coupling strength between subunits. It corresponds indirectly to the amount of associated FKBP with low values of s corresponding to nearly all FKBP being dissociated and high values of s corresponding to full FKBP association.

To include this interaction into the RyR gating dynamics, we need to specify how this interaction energy enters into the rate constants. Here, we simply follow Stern et al. (27) and let one-half of the energy contribute to the forward rate constant and the other-half to the backward rate constant. In other words, the rate constants $K_{\rm ij}$ for the transition from state i to state j have the form

$$K_{\rm ij} = k_{\rm ij} \exp\left(\sum \frac{s(\Delta E_{\rm is_m} - \Delta E_{\rm js_m})}{2kT}\right), \tag{8}$$

where the sum is over neighboring subunits and $s_{\rm m}$ is the state of the neighboring subunits. The values of matrix elements $\Delta E_{\rm ij}$ and the transition rates $k_{\rm ij}$ in the absence of any allosteric interaction used in our simulations are given in Table 2.

Based on experimental results, we take the number of RyRs in our basic calcium-release unit to be 100 (28). Fast equilibrium of calcium diffusion within the dyadic space is assumed so that all the RyRs in the same calcium-release unit sense $[Ca^{2+}]_{\rm ds}$ with no difference. The total flux through the RyRs in a CRU is then proportional to the concentration gradient and the number of open subunits, $N_{\rm open,RyR}$,

TABLE 2 RyR parameters

Parameter	Description	Value
$N_{\rm RyR}$	Number of RyRs in a CaRU	100
$g_{\rm RyR}$	Conductance of single RyR subunit	800/s
$k_{\rm co}$	Transition rate from C to O	31.25 μM/s
$k_{\rm oc}$	Rate constant from O to C	1250.0/s
$k_{\rm oi}$	Rate constant from O to I	5.0/s
$k_{\rm io}$	Rate constant from I to O	5.0/s
$k_{\rm ic}$	Rate constant from I to C	0.5/s
$k_{\rm ci}$	Rate constant from C to I	0.05 μM/s
$\Delta E_{\rm co}$	Interaction energy between C and O	5.0 kT
$\Delta E_{\rm oi}$	Interaction energy between O and I	1.667 kT
$\Delta E_{\rm ci}$	Interaction energy between C and I	0
s	Strength of coupling between subunits	Adjustable

$$J_{\rm RyR} = g_{\rm RyR} N_{\rm open,RyR} ([Ca^{2+}]_{\rm jSR} - [Ca^{2+}]_{\rm ds}), \tag{9}$$

where $g_{\rm RyR}$ is the conductance of a single RyR subunit. See Table 2 for parameter settings.

The E-C coupling gain

The E-C coupling gain function is defined as

$$Gain = \frac{J_{\rm RyR,max} - J_{\rm RyR,rest}}{J_{\rm dhpr,max}}, \tag{10}$$

where $J_{\rm RyR,\,max}$ and $J_{\rm dhpr,\,max}$ are the maximal fluxes through the RyR cluster and the L-type calcium channels during E-C coupling, and $J_{\rm RyR,\,rest}$ is the calcium release through the RyR receptors in the absence of $J_{\rm dhpr}$.

Simulation protocol

The gating of L-type calcium channels and RyRs are simulated as Markov processes. Thus, at each time step, a random number is generated to help a channel to decide how its state should change based on the rate equations. The time step Δt is set to be 10^{-5} s, which is much shorter than all the processes except the calcium efflux from dyadic space to the cytoplasm. During Δt, Eq. 1 is integrated analytically under the approximation that $J_{\rm dhpr}$, $J_{\rm RyR}$, and $J_{\rm Buf}$ do not change during such a short time-interval. Equation 3 is simply integrated using Euler's method.

All simulations reported here consisted of presenting a sequence of triggers to the CRU. The trigger, given once every second, consisted of clamping the membrane voltage from a holding voltage of −80 mV to a specified higher potential (0 mV everywhere, except in Fig. 2 where it is varied) for a duration of 0.1 s. Since each CRU exhibits a response that varies stochastically from trigger to trigger, this sequence needs to be long enough to ensure statistically meaningful results that can be compared to the spatially averaged results in myocyte experiments. In all simulations recorded here, we used a sequence of 1000 triggers, with the first 50 discarded to eliminate transient effects.

In our simple model, in which the nSR calcium concentration is kept constant, it is sufficient to simulate a single release unit. In the full model, on the other hand, we simulated 100 CRUs simultaneously. Each release unit shares a common cytoplasm and nSR, in which the calcium concentration is treated as a dynamic variable. Further details are furnished in the Supplementary Material.

RESULTS

We start by showing in Fig. 2 the gain as a function of the membrane potential for a particular value of s. For different values of s, we obtained qualitatively similar curves (data not

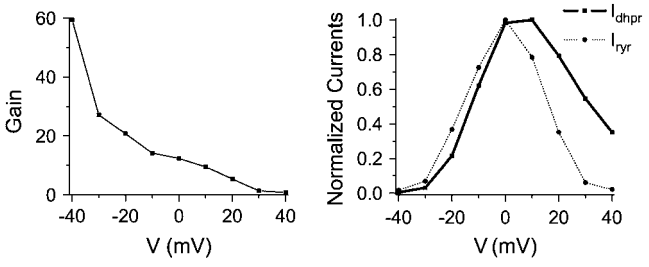

FIGURE 2 (*Left*) The E-C coupling gain as a function of the membrane voltage. (*Right*) The current through the L-type channel and the RyR, both normalized to their peak values, is a function of the membrane voltage. The value s is set to be 0.5 in this simulation.

shown). The gain is clearly a monotonically decreasing function of the membrane potential and displays the graded release found in experiments (29–31). The current through a single L-type channel and through a RyR, on the other hand, is bell-shaped, with a small difference between their positions. This type of graded release is indicative of the local control theory. After all, if the RyR would respond only to the ensemble-averaged L-type current it would be impossible to have a different gain for two identical values of I_{dhpr}. Instead, the RyR responds to and is triggered by local L-type channels.

We next show in Fig. 3 the calcium concentration in the dyadic space as a function of time for different values of s. As s is increased, the decay rate becomes larger and the peak calcium concentration increases. After $s \sim 0.4$, however, both the decay time and the rising rate increase and this peak calcium concentration decreases. This leads to a maximum in peak calcium concentration for a particular value of the cooperativity parameter $s^* \sim 0.4$.

The gain function also shows a clear maximum as a function of the cooperativity s (Fig. 4 *A*) with the maximum occurring at $s = s^*$. Here, as in Fig. 4, *B* and *C*, we have plotted the results from the simple model as a thick solid line and the results from the full model as a thin dashed line. Further characterization of the effect of a varying s is illustrated in Fig. 4 *B* where we plot the diastolic jSR content as function of s. The diastolic jSR content was measured during the second-half of the 1-s interval separating the stimuli. This content increases monotonically until $s \sim s^*$, and then reaches the nSR concentration in the simple model. In the full model, on the other hand, the jSR content depends on the uptake mechanisms and reaches an equilibrium for larger values of s. The resting value of the calcium concentration in the dyadic space as a function of s is plotted in Fig. 4 *C*. It is a monotonically decreasing function of s for $s < s^*$ and is roughly constant for $s > s^*$.

Comparing the results from the two models shows that the simple model already captures the essential qualitative features of the full model. It also shows a distinct bell-shaped gain curve, while the jSR content saturates at slightly earlier values of s. Note that the calcium concentration in the dyadic space in the full model increases more slowly when s is decreased due to the partial depletion of the jSR and the nSR. Finally, the nSR calcium concentration in the full model follows the jSR calcium concentration for $s > s^*$ and decreases to values slightly higher than the jSR calcium concentration for $s > s^*$ (data not shown). In the remainder of the article, we will focus on the simple model.

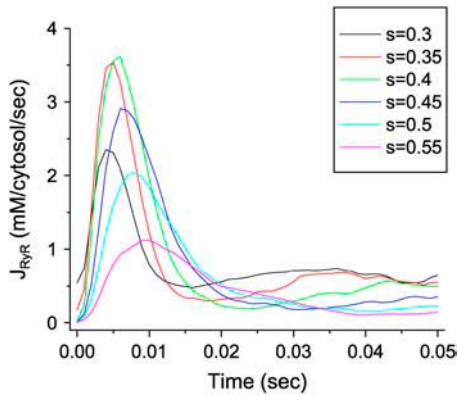

FIGURE 3 Calcium release through the RyR cluster in the dyadic space for different values of s following a 0.1-s pulse of the membrane potential started at $t = 0$ s. The release reaches its maximum at $s = 0.4$.

The reduced SR content for $s < s^*$ is caused by an increased leak in the RyR. This is shown in Fig. 5 *A*, where we have plotted the open probability P_0 as a function of background calcium for two different values of s. This probability is calculated analytically and represents the probability that at least one subunit is open. Reducing the cooperativity leads to a shift in this curve to smaller values of calcium and thus to an increased probability for opening at low calcium concentration. The presence of an increased leak is further illustrated in Fig. 5, *B* and *C*, where we plot the distribution of open states within an RyR at a controlled calcium concentration (the *dashed line* in Fig. 5 *A*). For $s = 0$ (Fig. 5 *B*), the subunits are completely independent and the distribution shows a significant contribution from the subconductance states. For high values of s (Fig. 5 *C*), the increased cooperativity suppresses the subconductance states and the fully closed and fully open states become dominant.

The effect of the subunit cooperativity and the presence of a leak can be further characterized by the spontaneous spark frequency. To measure this frequency, we stimulated the cell every second and measured the number of sparks 0.5 s before each stimulus. The total duration of the numerical experiment was 50 s, and to ensure the steady state was reached, we discarded the first 40 s. We defined a spontaneous calcium spark as an event during which 30% or more of the subunits open. Furthermore, to prevent counting small fluctuations around this threshold value, we required the activity to decrease below 5% of the subunits before a new spark could be counted. The measured spark frequency (per CRU) is shown in Fig. 6 and shows that this frequency decreases rapidly when s approaches s^*. For $s > s^*$, the measured spontaneous spark frequency was essentially zero, indicating that an increased cooperativity reduces the probability for a spontaneous spark and hence for leak. Furthermore, assuming a distance of 2 μm between CRUs along a *Z*-line, for s slightly smaller than s^* we obtain spark rates (0.1–0.5/s/CRU) that are in good agreement with experimentally obtained values (0.1 /s/CRU) (14).

We have also examined the detailed calcium-release pattern in the presence of the L-type channel current and found it was different for $s < s^*$ and $s > s^*$. In Fig. 7 *A*, we plot the distribution of latency times, defined as the time between the rising of the test potential and the time when J_{RyR} reaches its maximum. As s is increased, the average and the variation of the latency times are:

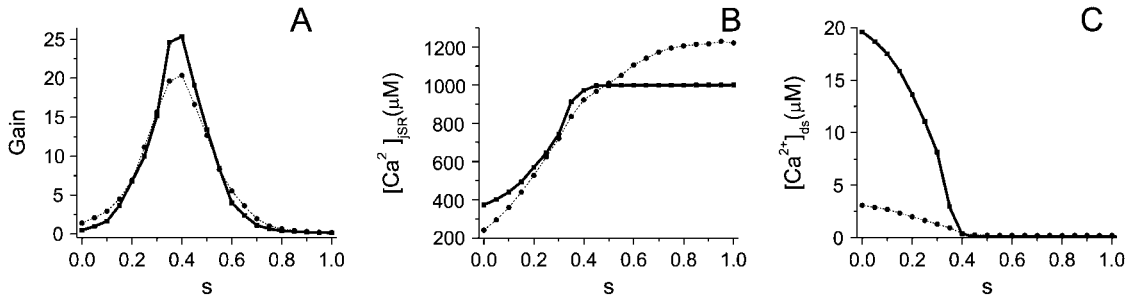

FIGURE 4 Dependence of the gain (*A*), the resting jSR calcium level (*B*), and the diastolic calcium concentration in the dyadic cleft (*C*) on the coupling strength (s). The thick lines show results from the simple model and the thin lines display results from the full model (see Supplementary Material).

7.9 ms and 8.2 ms, respectively, for $s = 0.3$ ms;
7.6 ms and 4.9 ms, respectively, for $s = 0.4$; and
13.3 ms and 8.5 ms, respectively, for $s = 0.5$.

The mean latency time increases significantly when $s > s^*$, and the variation reaches minimum at $s = s^*$. Furthermore, we have calculated the total fraction of open RyR channel subunits within a cluster at the peak calcium concentration, and have plotted its distribution in Fig. 7 *B*. As s is increased, this distribution changes from essentially single-peaked to clearly double-peaked. In other words, for higher values of s, the probability of opening becomes smaller and a substantial portion of clusters exhibit a small fraction of open RyRs. This, combined with the larger variation in latency time, indicates that the calcium release from different clusters is less synchronized by the triggers when the cooperativity becomes larger than s^*.

To examine the dependence of the gain on the SR load, we also performed simulations using a higher nSR calcium concentration and recalculated the gain as a function of s. The result, for two different values of $[Ca^{2+}]_{nSR}$, is plotted in Fig. 8 and shows that the qualitative form of the gain curve has not changed. On the other hand, the peak value of the gain shifts toward lower values of s for increased SR content. Thus, for a given value of s, the gain function can be either increasing or decreasing, depending on the value of the SR load.

DISCUSSION

In this article, we have examined the effect of cooperativity between RyR subunits using a theoretical approach. This approach consists of modeling the calcium dynamics within the cell and the dyadic cleft combined with a novel Markovian approach for the RyR. The RyR Markovian model takes into account the subunit structure of the RyR and includes a measure of cooperativity s. Using this model, we calculated the E-C coupling gain as a function of several system parameters. Our main result is that this gain exhibits a clear maximum for a particular value of the cooperativity, $s = s^*$. For larger cooperativity values, the resting jSR content is s-insensitive, whereas for smaller values it decreases with decreasing s.

To understand intuitively why the gain curve displays a maximum, let us consider the effects of the subunit cooperativity s on the gain. This gain is roughly determined by the maximum value of J_{RyR} and is thus given by the product of the open probability of the RyRs and the gradient of the calcium concentration between the jSR and the dyadic space (see Eq. 9). Increasing s decreases the open probability, but it increases the calcium concentration difference between the jSR and the dyadic space due to the suppression of subconductance states of the RyR. The competition of these two opposite effects leads to a maximum of gain at some definite s^*.

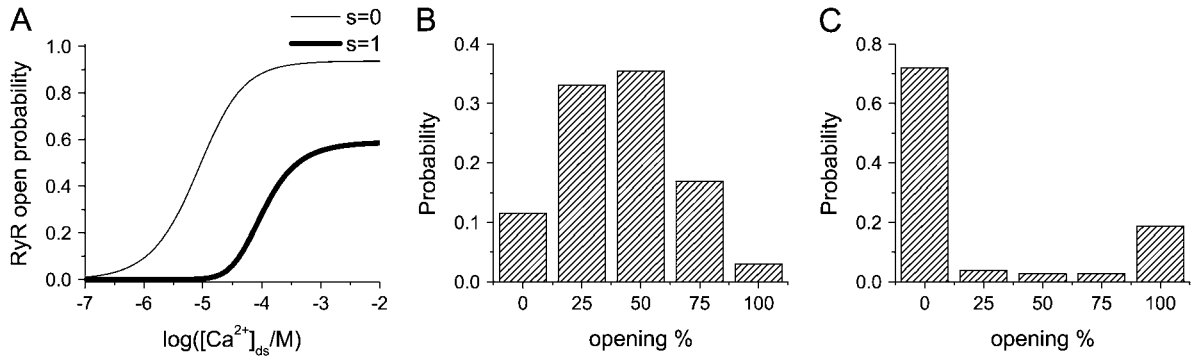

FIGURE 5 (*A*) The probability of opening as a function of the background calcium concentration for two different values of s. (*B* and *C*) The probability of opening for each of the five possible RyR configurations for $s = 0$ (*B*) and $s = 1$ (*C*). The background calcium concentration is held fixed at 100 μM (shown as *dashed line* in *A*).

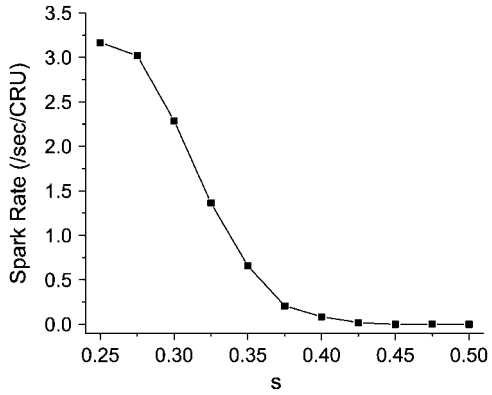

FIGURE 6 The spontaneous spark frequency as a function of the cooperativity s. There is very severe leak when s is small, and almost no sparks when $s > s^*$.

Specifically, for $s > s^*$, upon recalling that increasing s represents an energy penalty for a subunit to be in a different state than its neighbors, it is easy to see that a large s makes it more difficult to have fractional openings. In other words, the RyR subunits become more likely to open and close collectively and leads to a smaller effective activation rate due to a higher energy barrier between closed and open states. This can be seen from Fig.7 *A*, which shows that the latency time increases as s is increased. Thus, the probability that a cluster can be triggered to open successfully is reduced, which leads to a reduced gain.

For $s < s^*$, the probability that the RyRs exhibit subconductance states becomes substantial (Fig. 5). This leads to a persistent SR leak during diastole, defined here as one-half second before a stimulus. This causes a decreased SR content (Fig. 4 *B*) and an increased diastolic calcium level in the dyadic space (Fig. 4 *C*). Hence, upon an I_{dhpr} stimulus, the calcium current through the RyRs is smaller, leading to a decreased E-C coupling gain.

How do these results relate to experimental findings? As discussed above, our cooperativity parameter s correlates with the amount of FKBP associated with the RyR complexes in the cell. The effect of FKBP on in vivo E-C coupling has been investigated in three species: rat, mouse, and rabbit. For the latter, FKBP sequestering reduced E-C coupling (12), while FKBP overexpression increased E-C coupling (13,14). In rats and mice, on the other hand, FKBP sequestering increased E-C coupling (10–12), even though overexpression appears to increase E-C coupling (15). These results appear to be contradictory, although there are, of course, caveats about whether other components of the calcium-handling system are affected by the different protocols. If, for the moment, we ignore the data from FKBP overexpression in rats, we can combine all the other experimental data with the results of our theoretical modeling and provide the following hypothesis: normal levels of cooperativity in rats and mice are higher than the optimal level, while normal levels of cooperativity in rabbits are lower than the optimal level. One way to achieve this difference is schematically drawn in Fig. 9 *A*, where the circle represents the postulated

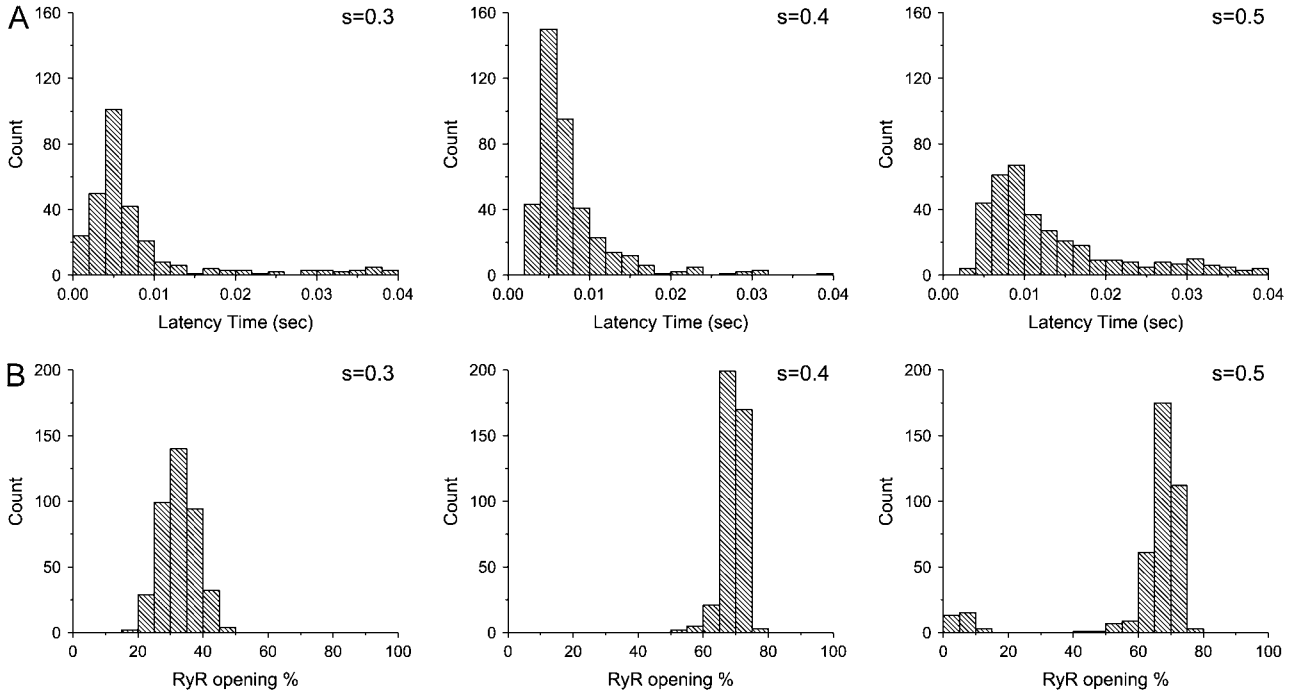

FIGURE 7 (*A*) The distributions of the latency time of the release triggered by the L-type channel current with varied levels of cooperativity. (*B*) The corresponding distributions of the peak opening fraction during the release triggered by the L-type channel current.

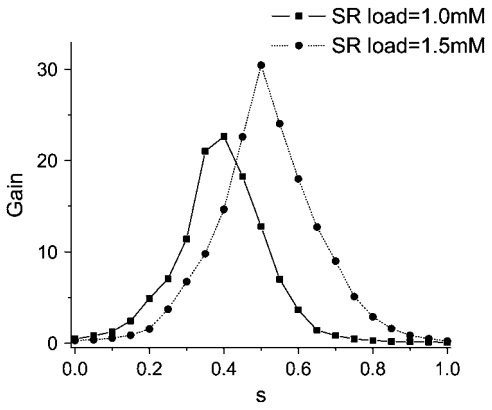

FIGURE 8 The gain as a function of the cooperativity for two different fixed values of the SR content.

operating point for rats and mice and the square represents rabbits. Another possibility, of course, is that the subunit cooperativity across species is preserved, while other factors determining the gain vary. Then, as is schematically shown in Fig. 9 *B*, the rabbit gain curve has shifted in its entirety toward higher values of s compared to the gain curve for the rat and mouse (or vice versa), while the value of the cooperativity s_{op} is the same for both species. In both cases, the operating value of s for the rat and mouse is larger than s^*, which agrees with experimental data showing that the SR content is maintained during FKBP dissociation (12). The fact that the SR content decreases in rabbits after dissociation of FKBP and increases after FKBP overexpression (12,13) serves as a self-consistency check (see Fig. 4).

On the other hand, if the overexpression of FKBP in rats does indeed increase the E-C coupling gain (15), we have to modify the above hypothesis. In this case, the experimental data is consistent with our modeling results if we assume that both rats/mice and rabbits have a normal level of cooperativity that is lower than the optimal level. Of course, this still leaves open the question why FK506 decreases the gain in rats but perhaps, as pointed out in Gomez et al. (15), it also acts on other components of the E-C coupling machinery. In summary, it is clear that rabbits lie to the left of the peak and the situation for rats/mice needs to be clarified experimentally.

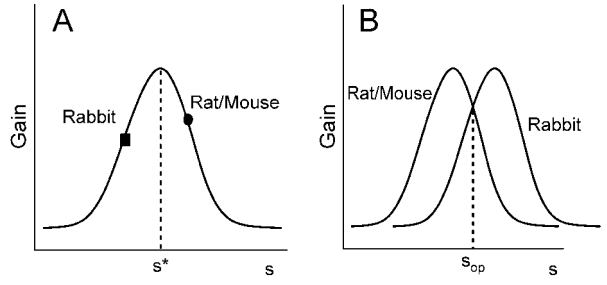

FIGURE 9 Possible schematic E-C coupling gain as a function of the FKBP association. (*A*) The gain function is the same for different species although the cooperativity level varies. As noted on the figure, the postulated operating point for rabbits is marked by a square, and the operating point for mice and rats is marked by a circle. (*B*) The cooperativity is the same across species, although the gain function is different.

Another comparison comes from the distribution of the spark latency times. Two groups (32,33) performed experiments showing that the calcium release is more synchronized under β-AR stimulation. Although Song and co-workers hypothesized that the observed simultaneous release of calcium is mainly an effect of increased L-type channel current, we show in Fig. 7 that a decreased cooperativity inside RyR can also cause a larger probability for a cluster to respond to the trigger. Moreover, our model predicts that the mean latency time increases as s increases, which is consistent with experiments (32).

A final comparison with in vivo experiments can be made when we analyze the frequency of spontaneous sparks (Fig. 6). Since increasing s corresponds to increasing the energy barrier, we find that the spark frequency decreases as s increases. This is consistent with experimental findings that show a decreased spontaneous spark frequency in rabbits with overexpressed FKBP (14). In fact, it is also consistent with the observed decrease in spontaneous spark frequency in FKBP-overexpressing rats (15), independent of the aforementioned uncertainty as to the normal level of cooperativity. In addition, the model shows that for $s < s^*$, the total released calcium in a cluster is smaller than for $s \sim s^*$ due to a decreased jSR content. Thus, for $s < s^*$ a locally triggered spark is less likely to initiate a release event in the neighboring cluster and a propagating wave is more likely to abort. This scenario seems consistent with experimental data in FKBP-overexpressed rabbits. Of course, to investigate wave propagation in our model requires us to include spatial coupling between cluster and t-tubules. Once incorporated, this model would then be able to investigate the stochastic process of wave abortion, using a similar approach to that employed in Falcke et al. (34) for the case of *Xenopus* oocytes.

Our major goal was to produce a model that could be compared with data from single myocyte studies as well as from bilayer experiments. The bilayer experiments suggest that in the presence of FKBP the subconductance states are nearly completely suppressed, whereas in the absence of FKBP they are prominently present. By assuming that each RyR subunit can contribute one-quarter of the total conductance independently and that they must act cooperatively with FKBP binding, our model produces very similar distributions of subconductance states (Fig. 5), as shown in those experiments.

Our model is not able to investigate the complete fight-or-flight response, during which the β-adrenergic pathway is stimulated and PKA activation levels are elevated. This signaling pathway not only targets the RyR but also increases the influx through the L-type channel and the calcium uptake through the SERCA pumps, mechanisms that are not included in our study. Nevertheless, if our hypothesis shown in Fig. 9 is

correct, we can postulate that the relative importance of the components involved in the fight-or-flight response should be species-dependent. After all, independent of the species, the net result of the fight-or-flight response is an increased E-C coupling gain and cardiac output (35). If our postulated schematic gain function in Fig. 9 is correct, β-adrenergic stimulation in rabbits will reduce the E-C coupling gain if only considering the dissociation of FKBP from RyR. Thus, one of the other targets of β-adrenergic pathway needs to compensate the reduction of gain associated with the loss in cooperativity. In mice and rats, if we assume that FK-506 acts primarily on RyRs to decrease the cooperativity and increase the E-C coupling gain, this compensation is not necessary. Of course, if both rabbits and rats operate with normal levels of s below the maximal value, rats also need a compensatory mechanism.

The effect of FKBP dissociation on human congestive heart failure, and in particular the role of PKA hyperphosphorylation, is a controversial topic. Several groups have found that the FKBP association level is significantly decreased by PKA hyperphosphorylation in HF myocytes (19,21). Furthermore, experiments have shown that drugs can prevent the onset of experimental heart failure by reversing PKA hyperphosphorylation and preventing the decrease of RyR-bound FKBP (21). Other groups, however, have reported that PKA hyperphosphorylation of RyR does not dissociate FKBP from RyR and cannot influence RyR function (36–38). Our model does not take into account the actual mechanism whereby the cooperativity is changed and, hence, cannot shed light on the hyperphosphorylation controversy. On the other hand, our model shows that a scenario in which partial association of FKBP (i.e., a slightly lower value of s) results in an increased E-C coupling and severe dissociation of FKBP (i.e., a very low value of s) leads to events typically associated with heart failure (reduced SR content, decreased ECC gain, and increased diastolic leak) is, in fact, plausible.

Our model to-date is quite useful, but can clearly be extended. For example, we have only modeled the effect of FKBP on the coupling between the RyR subunits. There is experimental evidence, however, that FKBP can also couple neighboring receptors (39,40). Several groups have addressed the effect of receptor-receptor coupling on calcium dynamics. A recent modeling study, which implements coupling between neighboring RyRs in much the same way as we do here, found that introducing a cooperativity between receptors can make certain unstable RyR gating schemes stable (27). Another modeling study showed that a lack of cooperativity between receptors can lead to prolonged calcium sparks (24). In our model, we also observed an increase in the duration of these sparks when we lowered s (data not shown). In fact, we believe that the inter-receptor coupling discussed in Sobie et al. (24) and Stern et al. (27) and the intra-receptor coupling discussed in this article may lead to very similar effects. For example, we predict that the gain curve will exhibit a similar qualitative form when varying the inter-receptor coupling constant. The relative importance of intra- versus inter-receptor coupling remains to be resolved.

To circumvent the above-mentioned limitations, a spatially extended model of the calcium dynamics that includes cooperativity between neighboring RyRs, coupled to a detailed electrophysiological model, needs to be developed. Such an undertaking is computationally very challenging and beyond the scope of this study. Finally, there is no way to date to establish a quantitative link between the concentration of FKBP and the value of s. This would require direct measurements of the gating mechanisms while varying the FKBP concentration.

SUPPLEMENTARY MATERIAL

An online supplement to this article can be found by visiting BJ Online at http://www.biophysj.org.

Y.T. acknowledges the hospitality of the Center for Theoretical Biological Physics.

This work was supported by the National Science Foundation-sponsored Center for Theoretical Biological Physics, grant No. PHY-0216576 and grant No. 0225630 to K.W., W.J.R., and H.L.; and by National Institutes of Health RO1 grant No. HL075515 to W.J.R.

REFERENCES

1. Bers, D. 2001. Excitation-Contraction Coupling and Cardiac Contractile Force. Kluwer, Boston, MA.
2. Hasenfuss, G., and B. Pieske. 2002. Calcium cycling in congestive heart failure. *J. Mol. Cell. Cardiol.* 34:951–969.
3. Sjaastad, I., J. A. Wasserstrom, and O. M. Sejersted. 2002. Heart failure—a challenge to our current concepts of excitation-contraction coupling. *J. Physiol.* 546:33–47.
4. Parker, M. 1985. Sudden unexpected death in patients with congestive heart failure: a second frontier. *Circulation.* 72:681–685.
5. Bers, D. 2000. Calcium fluxes involved in control of cardiac myocyte contraction. *Circ. Res.* 87:275–281.
6. Bers, D. M., D. A. Eisner, and H. H. Valdivia. 2003. Sarcoplasmic reticulum Ca^{2+} and heart failure: roles of diastolic leak and Ca^{2+} transport. *Circ. Res.* 93:487–490.
7. Marks, A. R. 2003. A guide for the perplexed: towards an understanding of the molecular basis of heart failure. *Circulation.* 107:1456–1459.
8. Brillantes, A. B., K. Ondrias, A. Scott, E. Kobrinsky, E. Ondriasova, M. C. Moschella, T. Jayaraman, M. Landers, E. E. Ehrlich, and A. R. Marks. 1994. Stabilization of calcium release channel (ryanodine receptor) function by FK506-binding protein. *Cell.* 77:513–523.
9. Ahern, G. P., P. R. Junankar, and A. F. Dulhunty. 1997. Subconductance states in single-channel activity of skeletal muscle ryanodine receptors after removal of FKBP12. *Biophys. J.* 72:146–162.
10. McCall, E., L. Li, H. Satoh, T. R. Shannon, L. A. Blatter, and D. M. Bers. 1996. Effects of FK-506 on contraction and Ca^{2+} transients in rat cardiac myocytes. *Circ. Res.* 79:1110–1121.
11. Xin, H. B., T. Senbonmatsu, D. S. Cheng, Y. X. Wang, J. A. Copello, G. J. Ji, M. L. Collier, K. Y. Deng, L. H. Jeyakumar, M. A. Magnuson, T. Inagami, M. I. Kotlikoff, and S. Fleischer. 2002. Oestrogen protects FKBP12.6 null mice from cardiac hypertrophy. *Nature.* 416:334–338.
12. Su, Z., K. Sugishita, F. Li, M. Ritter, and W. H. Barry. 2003. Effects of FK506 on $[Ca^{2+}]_i$ differ in mouse and rabbit ventricular myocytes. *J. Pharmacol. Exp. Ther.* 304:334–341.

13. Prestle, J., P. M. Janssen, A. P. Janssen, O. Zeitz, S. E. Lehnart, L. Bruce, G. L. Smith, and G. Hasenfuss. 2001. Overexpression of FK506-binding protein FKBP12.6 in cardiomyocytes reduces ryanodine receptor-mediated Ca^{2+} leak from the sarcoplasmic reticulum and increases contractility. *Circ. Res.* 88:188–194.

14. Loughrey, C. M., T. Seidler, S. L. Miller, J. Prestle, K. E. MacEachern, D. Reynolds, G. Hasenfuss, and G. L. Smith. 2004. Over-expression of FK506-binding protein FKBP12.6 alters E-C coupling in adult rabbit cardiomyocytes. *J. Physiol.* 556:919–934.

15. Gomez, A. M., I. Schuster, J. Fauconnier, J. Prestle, G. Hasenfuss, and S. Richard. 2004. FKBP12.6 overexpression decreases Ca^{2+} spark amplitude but enhances $[Ca^{2+}]_i$ transient in rat cardiac myocytes. *Am. J. Physiol. Heart Circ. Physiol.* 287:H1987–H1993.

16. Hain, J., H. Onoue, M. Mayrleitner, S. Fleischer, and H. Schindler. 1995. Phosphorylation modulates the function of the calcium release channel of sarcoplasmic reticulum from cardiac muscle. *J. Biol. Chem.* 270:2074–2081.

17. Valdivia, H. H., J. H. Kaplan, G. C. Ellis-Davies, and W. J. Lederer. 1995. Rapid adaptation of cardiac ryanodine receptors: modulation by Mg^{2+} and phosphorylation. *Science.* 267:1997–2000.

18. Marks, A. R., S. Reiken, and S. O. Marx. 2002. Progression of heart failure: is protein kinase A hyperphosphorylation of the ryanodine receptor a contributing factor? *Circulation.* 105:272–275.

19. Marx, S. O., S. Reiken, Y. Hisamatsu, T. Jayaraman, D. Burkhoff, N. Rosemblit, and A. R. Marks. 2000. PKA phosphorylation dissociates FKBP12.6 from the calcium release channel (ryanodine receptor): defective regulation in failing hearts. *Cell.* 101:365–376.

20. Ono, K., M. Yano, T. Ohkusa, M. Kohno, T. Hisaoka, T. Tanigawa, S. Kobayashi, M. Kohno, and M. Matsuzaki. 2000. Altered interaction of FKBP12.6 with ryanodine receptor as a cause of abnormal Ca^{2+} release in heart failure. *Cardiovasc. Res.* 48:323–331.

21. Yano, M., S. Kobayashi, M. Kohno, M. Doi, T. Tokuhisa, S. Okuda, M. Suetsugu, T. Hisaoka, M. Obayashi, T. Ohkusa, M. Kohno, and M. Matsuzaki. 2003. FKBP12.6-mediated stabilization of calcium-release channel (ryanodine receptor) as a novel therapeutic strategy against heart failure. *Circulation.* 107:477–484.

22. Wehrens, X. H., S. E. Lehnart, F. Huang, J. A. Vest, S. R. Reiken, P. J. Mohler, J. Sun, S. Guatimosim, L. S. Song, N. Rosemblit, J. M. D'Armiento, C. Napolitano, M. Memmi, S. G. Priori, W. J. Lederer, and A. R. Marks. 2003. FKBP12.6 deficiency and defective calcium release channel (ryanodine receptor) function linked to exercise-induced sudden cardiac death. *Cell.* 113:829–840.

23. Wehrens, X. H., S. E. Lehnart, S. R. Reiken, S. X. Deng, J. A. Vest, D. Cervantes, J. Coromilas, D. W. Landry, and A. R. Marks. 2004. Protection from cardiac arrhythmia through ryanodine receptor-stabilizing protein calstabin2. *Science.* 304:292–296.

24. Sobie, E. A., K. W. Dilly, J. dos Santos Cruz, W. J. Lederer, and M. S. Jafri. 2002. Termination of cardiac Ca^{2+} sparks: an investigative mathematical model of calcium-induced calcium release. *Biophys. J.* 83:59–78.

25. Greenstein, J. L., and R. L. Winslow. 2002. An integrative model of the cardiac ventricular myocyte incorporating local control of Ca^{2+} release. *Biophys. J.* 83:2918–2945.

26. Iyer, V., R. Mazhari, and R. L. Winslow. 2004. A computational model of the human left-ventricular epicardial myocyte. *Biophys. J.* 87:1507–1525.

27. Stern, M. D., L. S. Song, H. Cheng, J. S. Sham, H. T. Yang, K. R. Boheler, and E. Rios. 1999. Local control models of cardiac excitation-contraction coupling. A possible role for allosteric interactions between ryanodine receptors. *J. Gen. Physiol.* 113:469–489.

28. Franzini-Armstrong, C., F. Protasi, and V. Ramesh. 1999. Shape, size, and distribution of Ca^{2+} release units and couplons in skeletal and cardiac muscles. *Biophys. J.* 77:1528–1539.

29. Wier, W. G., T. M. Egan, J. R. Lopez-Lopez, and C. W. Balke. 1994. Local control of excitation-contraction coupling in rat heart cells. *J. Physiol.* 474:463–471.

30. Cannell, M. B., H. Cheng, and W. J. Lederer. 1995. The control of calcium release in heart muscle. *Science.* 268:1045–1049.

31. Janczewski, A. M., H. A. Spurgeon, M. D. Stern, and E. G. Lakatta. 1995. Effects of sarcoplasmic reticulum Ca^{2+} load on the gain function of Ca^{2+} release by Ca^{2+} current in cardiac cells. *Am. J. Physiol.* 268:H916–H920.

32. Song, L. S., S. Q. Wang, R. P. Xiao, H. Spurgeon, E. G. Lakatta, and H. Cheng. 2001. Beta-adrenergic stimulation synchronizes intracellular Ca^{2+} release during excitation-contraction coupling in cardiac myocytes. *Circ. Res.* 88:794–801.

33. Viatchenko-Karpinski, S., and S. Gyorke. 2001. Modulation of the Ca^{2+}-induced Ca^{2+} release cascade by β-adrenergic stimulation in rat ventricular myocytes. *J. Physiol.* 533:837–848.

34. Falcke, M., L. Tsimring, and H. Levine. 2000. Stochastic spreading of intracellular Ca^{2+} release. *Phys. Rev. E.* 62:2636–2643.

35. Wherens, X. H. T., and A. R. Marks. 2003. Altered function and regulation of cardiac ryanodine receptors in cardiac disease. *Trends Biochem. Sci.* 28:671–678.

36. Li, G., C. Lau, A. Ducharme, J. Tardif, and S. Nattel. 2002. Transmural action potential and ionic current remodeling in ventricles of failing canine hearts. *Am. J. Physiol. Heart Circ. Physiol.* 283:H1031–H1041.

37. Jiang, M. T., A. J. Lokuta, E. F. Farrell, M. R. Wolff, R. A. Haworth, and H. H. Valdivia. 2002. Abnormal Ca^{2+} release, but normal ryanodine receptors in canine and human heart failure. *Circ. Res.* 91:1015–1022.

38. Xiao, B., C. Sutherland, M. P. Walsh, and S. R. W. Chen. 2004. Protein kinase A phosphorylation at serine-2808 of the cardiac Ca^{2+}-release channel (ryanodine receptor) does not dissociate 12.6-kDa FK506-binding protein (FKBP12.6). *Circ. Res.* 94:487–495.

39. Marx, S. O., K. Ondrias, and A. R. Marks. 1998. Coupled gating between individual skeletal muscle Ca^{2+} release channels (ryanodine receptors). *Science.* 281:818–821.

40. Marx, S. O., J. Gaburjakova, M. Gaburjakova, C. Henrikson, K. Ondrias, and A. R. Marks. 2001. Coupled gating between cardiac calcium release channels (ryanodine receptors). *Circ. Res.* 88:1151–1158.